Neoplasia 59 (2025) 101084

Contents lists available at ScienceDirect

Neoplasia

journal homepage: www.elsevier.com/locate/neo

Original Research

Engineering and characterization of Hu3A4: A novel humanized antibody with potential as a therapeutic agent against myeloid lineage leukemias

Sisi Li [a,†], Zhujun Wang [c,†], Xiaoping Guo [b], Yongmin Tang [b,*]

[a] School of Medicine, Hangzhou City University, #51 Huzhou Street, Hangzhou 310015, China
[b] Division of Hematology-Oncology, Pediatric Hematology-Oncology Center, Zhejiang Provincial Research Center for Childhood Leukemia New Diagnostic and Therapeutic Techniques, Children's Hospital, Zhejiang University School of Medicine, National Clinical Medical Research Center for Child Health, #57 Zhugan Road, Yan-an Street, Hangzhou 310006, China
[c] Department of Pediatrics, Union Hospital, Tongji Medical College, Huazhong University of Science and Technology, Wuhan, Hubei 430022, China

ARTICLE INFO

Keywords:
CD45RA
Humanized antibody
CDR grafting antibody
Leukemic stem cells
3A4
Targeting therapy

ABSTRACT

Leukemia stem cells (LSCs) play a critical role in the initiation, recurrence, and resistance to treatment of leukemia. Eradicating LSCs is crucial for the complete elimination of the disease. CD45RA is identified as an important marker for LSC subsets in acute myeloid leukemia (AML), providing a strategic target for therapy. In this report, we introduce Hu3A4, an innovative humanized CD45RA antibody devised to target LSCs expressing this antigen. Hu3A4 retains the antigen-recognition ability of its parental antibody while removing sequences from the variable region that could elicit human anti-mouse immune reactions. The modified variable regions of the heavy and light chains were intricately fused with the constant regions of human IgG1 heavy and light chains, respectively, producing a humanized antibody that emulates the structure of natural IgG. Hu3A4 was produced through recombinant expression in Chinese Hamster Ovary (CHO) cells, which ensured stable gene integration. In vitro tests revealed that Hu3A4 could effectively target and lyse the cells. Further, in vivo studies highlighted Hu3A4′s substantial anti-leukemic activity, significantly prolonging survival times in treated animal models compared to controls ($P < 0.01$). To summarize, Hu3A4 exhibits remarkable bioactivity and offers a promising therapeutic potential for the treatment of leukemia patients. Progressing Hu3A4 through additional preclinical and clinical studies is crucial to validate its efficacy as a therapeutic agent for leukemia.

Introduction

Leukemic stem cells (LSCs), characterized by their resistance to chemotherapy, capability for self-renewal, and pluripotency, play a crucial role in the initiation, persistence, and relapse of acute myeloid leukemia (AML) [1]. These cells are capable of regenerating the full array of leukemic cells seen in AML, thereby driving the disease's recurrence. This underscores the importance of LSCs as a prime target for therapeutic intervention [1,2].

The emergence of monoclonal antibodies has marked a significant advancement in precisely targeting specific antigens, including those found on LSCs [3]. This precision enables the development of targeted therapies aimed at the root causes of conditions like AML, heralding a new era of cancer treatment characterized by specificity and efficacy. The innovation in monoclonal antibody therapy begins with the exploration of the variable region (V region), essential for antigen specificity [4,5]. Techniques such as animal immunization [6], the creation and screening of human antibody gene libraries, and the single-cell culture with sequencing of human B cells are employed to identify candidates that bind specifically to antigens associated with the therapy's aim [5,7]. Monoclonal antibody drugs have occupied the largest share of the global biopharmaceutical market. By the end of 2021, 522 unique antigens had been targeted by at least one clinical-stage monoclonal antibody [8].

Monoclonal antibodies are categorized based on their immunogenicity into murine, chimeric, humanized, and fully human types. Murine monoclonal antibodies are entirely composed of mouse immunoglobulins [9]. Chimeric monoclonal antibodies, which are made by merging mouse with human antibodies, contain over 65 % human antibodies [10]. Humanized monoclonal antibodies, created by attaching mouse

* Corresponding author.
E-mail address: y_m_tang@zju.edu.cn (Y. Tang).
† These authors contributed equally to this work.

https://doi.org/10.1016/j.neo.2024.101084
Received 15 April 2024; Accepted 5 November 2024

complementary determinant regions (CDR) with modifications to human antibody frames and fragment of constant region, have >90 % human antibody content. Fully human monoclonal antibodies are 100 % derived from human sources, produced by incorporating mouse antibody genetic material into human antibodies, thus significantly reducing the risk of human anti-mouse antibody (HAMA) reactions [11]. The antibodies targeting specific antigens of LSCs play a vital role in minimizing leukemia relapse by directly targeting and eliminating the cells responsible for disease maintenance and spread. The focus on developing humanized monoclonal antibodies against LSCs represents a pivotal direction in research, striving to merge targeted effectiveness with minimized immunogenicity towards achieving curative outcomes in AML therapy [3,12]. Among various markers, CD45RA has been identified as a highly reliable marker for LSCs in the majority of AML patients, facilitating the LSC identification and quantification over other markers like CLL-1 (also known as CLEC12A), CD33, and CD123 [13, 14].

In our previous research, we successfully generated a new clone of mouse anti-human CD45RA monoclonal antibody 3A4 which recognizes the antigen on leukemic cells with high efficiency. Notably, 3A4 is rapidly internalized into target cells within 4 h. Furthermore, targeting with 3A4 conjugated with norcantharidin (NCTD-3A4) showed an exellent killing activity both in vitro and in animal models, making this antibody a potential therapeutic agent [15]. To further study the therapeutic potential of 3A4 against leukemia, we have also constructed a human-mouse chimeric antibody Hm3A4 [16] and its ranpirnase (Rap) conjugated immunotoxin Hm3A4-Rap [17]. Extensive testing in both laboratory and animal models has confirmed their exceptional ability to target and eradicate leukemia cells and LSCs.

To further investigate the targeted therapeutic effects of this antibody against leukemia, we applied Complementary-Determinant Region (CDR) grafting techniques for its humanization [18], resulting in the generation of a humanized antibody with a natural IgG1 conformation. Herein, we detail the preparation, biological activity, and both in vitro and in vivo anti-tumor effects of the humanized antibody.

Materials and methods

Cell lines and cell culture

KG1a cells (human acute myelogenous leukemia cell line, purchased from ATCC, Manassas, VA) were cultured in IMDM medium with 10 % (v/v) heat-inactivated fetal calf serum (FCS). CHO cells (purchased from ATCC, Manassas, VA) were cultured in RPMI 1640-Glutamax-I medium containing 10 % (v/v) heat-inactivated FCS. All cell lines were cultured in media supplemented with 100 units/ml of penicillin and 100 μg/ml streptomycin (Sangon Bioengineering Co., Shanghai, China) at 37 C in a humidified 5 % CO2 incubator.

Design and construction of eukaryotic expression vectors for humanized antibodies

Design of eukaryotic expression vectors

First, the variable region genes of the 3A4 light and heavy chains were aligned with the human antibody library using the online IMGT/V-QUEST tool to identify the most homologous sequences for humanization templates. The CDR regions of 3A4′s heavy and light chains were then grafted onto human templates, resulting in antibodies labeled as 3A4VHa (heavy chain) and 3A4VLa (light chain). Research indicates that the framework regions (FRs) of antibodies are crucial for CDR arrangement and antigen interaction, suggesting that simple CDR grafting can diminish antibody affinity [19]. To address this, we used Discovery Studio 2.5 to identify key amino acids within 5 angstroms of the CDR regions that influence the antibody's CDR conformation. We then reverted specific residues in the human FRs to their murine equivalents using molecular simulation to generate the mutated CDR-grafted antibody, aiming to produce high-affinity humanized antibodies labeled as 3A4VHb (heavy chain) and 3A4VLb (light chain). We compared the parental antibody sequences of 3A4VH, 3A4VL, and the back-mutated 3A4VHb and 3A4VLb with the human antibody library, evaluating the degree of humanization of the antibodies using z-scores [20] with the online software available at http://acrmwww.biochem.ucl.ac.uk/.

Construction of the eukaryotic expression vectors

Construction of the eukaryotic expression vectors for the humanized scFv. The entire genes of 3A4VHa, 3A4VLa, 3A4VHb, and 3A4VLb were synthesized. The scFv3A4a and scFv3A4b constructs were generated using splice-overlap extension PCR (SOE-PCR). Subsequently, the sequences of scFv3A4a and scFv3A4b sequences were individually cloned into TA cloning vectors, resulting in the creation of pGEM-T/scFv3A4a and pGEM-T/scFv3A4b, respectively. Subsequently, through double digestion and ligation, eukaryotic expression vectors pcDNA3.1/scFv3A4a and scFv3A4b were generated, capable of expressing humanized scFv proteins.

Construction of TA cloning vectors for human heavy chain constant region (CH) and light chain constant region (CL). Total RNA was extracted from peripheral blood mononuclear cells (PBMCs), and the human CH and CL segments were amplified via PCR. The resulting sequences were inserted into TA cloning vectors, yielding pGEM-T/CH and pGEM-T/CL, respectively.

Construction of the humanized heavy Chain Hu3A4VH-CH eukaryotic expression vector. The pHMCH3/3A4VHb and pGEM-T/CH vectors were digested with two restriction enzymes, and the target fragments were ligated to construct the Hu3A4VH-CH eukaryotic expression vector, labeled as pHMCH3/Hu3A4VH-CH.

Construction of the humanized light chain Hu3A4VL-CL eukaryotic expression vector. The pHMCH3/3A4VLb and pGEM-T/CL vectors were digested with two restriction enzymes, and the target fragments were ligated to construct the Hu3A4VL-CL eukaryotic expression vector, labeled as pHMCH3/Hu3A4VL-CL.

Expression and purification of the humanized antibody Hu3A4

Establishment of the stably transduced cell line Hu3A4s

CHO cells were co-transfected with pHMCH3/Hu3A4VH-CH and pHMCH3/Hu3A4VL-CL using lipofection. G418 selection was initiated 24 h post-transfection. After a 14-day period of G418 selection, immunofluorescence microscopy and flow cytometry were utilized to identify positive clones. These clones were subsequently subcloned three times to establish the stable cell line CHO/Hu3A4. All experimental procedures were performed according to previously published standard protocols [17].

Purification and molecular identity

Supernatants of CHO/Hu3A4 cells were harvested for the purification of Hu3A4 via Staphylococcal Protein A (SPA) affinity chromatography, and antibody concentrations were quantified using the Bicinchoninic Acid (BCA) assay. The presence and molecular weight of Hu3A4 in the culture supernatant were verified by SDS-PAGE and Western blot analyses, according to the standard protocol published previously [15].

Functional study of the humanized antibody Hu3A4

In evaluating the biological activity and function of Hu3A4, we concurrently utilized the chimeric scFv-Fc antibody as a control. This

approach further elucidates the advantages of a humanized antibody with a natural conformation.

The binding affinity

To assess and compare the binding affinity of Hu3A4, titration and competitive binding assays were performed according to the previously published standard protocol [16].

Titration assay. KG1a cells, harvested during their logarithmic growth phase, were adjusted to a concentration of 10^7/ml. Separate aliquots of 100 μl (10^6 cells) were then incubated with different concentrations of Hu3A4 and scFv3A4b-Fc (0.00125 μg, 0.0125 μg, 0.025 μg, 0.125 μg, 0.25 μg, 0.5 μg, 1.25 μg, 2.5 μg, and 5 μg) for 30 minutes at 25 °C in the dark to determine their binding affinities. Three replicate wells were performed for each condition. For detection, cells were further incubated with fluorescein isothiocyanate (FITC)-labeled goat anti-human Fc secondary antibody (GAHFc-FITC, KPL, Gaithersburg, MD) for 15 minutes at 25°C. Then the cells were washed twice with PBS before flow cytometry analysis (FCM) (FACSCalibur™, Becton Dickson, San Jose, CA, USA).

Competitive binding assay. A 100 μl aliquot (10^6 cells) of KG1a cell suspension was subsequently incubated with a fixed sub-saturating concentration of 0.5 μg 3A4-FITC, either alone or together with escalating doses of Hu3A4 and scFv3A4b-Fc, for 30 minutes at 25 °C. Additionally, a comparable concentration of mouse IgG1 isotype antibody was set as the control. Three replicate wells were performed for each condition. The stained cells were washed twice with PBS before FCM analysis, enabling the evaluation of competitive interactions and relative affinities.

In vitro targeting efficacy of Hu3A4 against KG1a cells

The cytotoxic effects of Hu3A4, relative to scFv3A4b-Fc, were evaluated on target cells using complement-dependent cytotoxicity (CDC) and antibody-dependent cellular cytotoxicity (ADCC) assays [17].

CDC. CDC assay was performed as described previously. Briefly, KG1a cells were washed and resuspended in serum-free RPMI-1640 at a concentration of 1×10^6 cells/ml. 50 μl of the cell suspension (5×10^4 cells) was added to each well of a 96-well plate, and then 25 μl of different concentrations (50 μg/ml, 25 μg/ml, 10 μg/ml) of Hu3A4 or scFv3A4b-Fc were added per well in triplicate and incubated for 1h. 25 μl of normal human serum (complement source) from healthy volunteers were added per well and incubated at 37 °C for 2 h. Wells with equal volumes of culture medium were used as the negative controls. 10 μl of CCK-8 (Beyotime Institute of Biotechnology, Shanghai, China) were added to each well and incubated for an additional 2 h at 37 °C.

To confirm the activity of the serum complement used, a verification was conducted with 2E8 (a mouse anti-human CD19 monoclonal antibody) reacting with B-ALL cell line Nalm-6 cells, which was previously confirmed by our laboratory. The experiment was setup as follows: ① Counted Nalm-6 cells and resuspended in serum-free RPMI-1640 to adjust the concentration to 1×10^6/ml. Seeding each well of a 96 well plate with 50 μl of the cell suspension, and using the aforementioned serum as the source of complement.② Using the medium as a negative control, 9 % Triton X-100 as a complete lysis control, and 25 μg/ml of 2E8 antibody with different amounts of serum complement (10 μl, 25 μl, and 50 μl) as the CDC detection groups.

The absorbance at 450 nm of the formazan dye produced by metabolically active cells from each well was measured using the Epoch 2 Microplate Spectrophotometer (BioTek, Winooski, Vermont, U.S.). Cytotoxicity was calculated based on the following formula:

$$\%\ of\ cytotoxicity = \frac{(C - E) - (T - E)}{(C - E)} \times\ 100\%$$

where C represents the absorbance of the medium group, E represents the absorbance of the complete lysis group, and T represents the absorbance of the experimental and control groups.

ADCC. The ADCC activities of Hu3A4 and scFv3A4b-Fc were evaluated using the CytoTox 96® Non-Isotopic Cell Killing Test Kit (Promega, Madison, Wisconsin, USA). Briefly, peripheral blood mononuclear cells (PBMC) were isolated from the blood of healthy volunteer by Ficoll-Hypaque separation (GE Healthcare/Amersham Biosciences) to be used as effector cells. Target cell suspensions were prepared by centrifuging log phase cells at 200g for 5 minutes, followed by washing twice with PBS and resuspending in phenol red-free RPMI-1640, adjusting the cell density to 3×10^5/ml. The Hu3A4 and scFv3A4b-Fc antibodies were then diluted to 0.1 mg/ml in phenol red-free RPMI-1640 medium. Target cells at adjusted densities were mixed with these antibody solutions, incubated at 4°C for 30 minutes, centrifuged at 200g for 5 minutes, washed twice with PBS, and resuspended in phenol red-free RPMI-1640. This suspension was then aliquoted 100 μl per well into a 96-well plate. Effector cells were added to each well at 100 μl, with effector to target ratios of 25:1 and 50:1. Three replicate wells were performed for each condition. The plate was incubated at 37°C in 5 % CO2 for 24 h before proceeding to color development. Following centrifugation at 200 *g* for 5 minutes, 50 μl of the supernatant from each well was transferred to a new 96-well plate. Subsequently, 50 μl of mixed substrate solution from the CytoTox 96® Non-Radioactive Cytotoxicity Assay Kit were added, incubated in the dark at room temperature for 30 minutes, and the absorbance at 490nm was read using a microplate reader.

In vivo antitumor efficacy of Hu3A4 in NOD/SCID Mice

To determine the *in vivo* antitumor activity of Hu3A4, we established a xenograft model by inoculating KG1a cells into non-obese diabetic (NOD)/severe combined immunodeficiency (SCID) mice. The establishment of the model was as follows: Twenty specific pathogen-free 4-week-old female NOD/SCID mice were purchased from Jiangsu Jicui Yaokang Biotechnology Co., Ltd (Jiangsu, China) and used for model generation and were assigned into four groups, 5 mice for each group (n=5): (1) the control group, (2) PBS treatment, (3) Hu3A4 treatment, and (4) scFv3A4b-Fc treatment groups. Mice were administered cyclophosphamide (CTX) by intraperitoneal injection 1 day prior to xenografting and were randomly assigned to the control or the xenograft group. The xenograft group which was further subdivided into the PBS, Hu3A4, and scFv3A4b-Fc treatment groups. All procedures complied with the requirements of the Institutional Animal Care and Usage Committee of Zhejiang University (approval ID: 2013-GJ-010).

On day 0 of the study, 1×10^6 exponentially growing KG1a cells in 100 μl or an equal volume of PBS were injected via the tail vein into the xenograft group or the control group, respectively. For the xenograft group, mice were treated intravenously with PBS, Hu3A4, or scFv3A4b-Fc on d1, d4, and D7, respectively. Disease symptoms (ruffled coat, hunched back, weakness, and reduced motility) were monitored daily. Mice with disease symptoms were sacrificed by cervical dislocation. The overall survival rate between the groups was statistically analyzed using the Kaplan-Meyer method.

Statistics

In vitro data were analyzed using a t-test. In vivo data between the groups was analyzed using the Kaplan-Meier method. $P < 0.05$ was considered to be statistically significant.

Results

Design of humanized antibodies and construction of their eukaryotic expression vectors

We identified the most homologous humanization templates: X62106 and X86355 for 3A4VH, and M23090 and AF103571 for 3A4VL. Then we modeled 3A4VH and 3A4VL's 3D structure and optimized them structurally and energetically to achieve the final 3D structures of the heavy and light chains by Discovery Studio 2.5 (Fig. 1). The z-score for 3A4VHb (-1.290) and 3A4VLb (-0.283) are higher than those for 3A4VH (-1.570) and 3A4VL (-1.804), respectively, indicating a significant increase in humanization with beneficial modifications (Fig. 2).

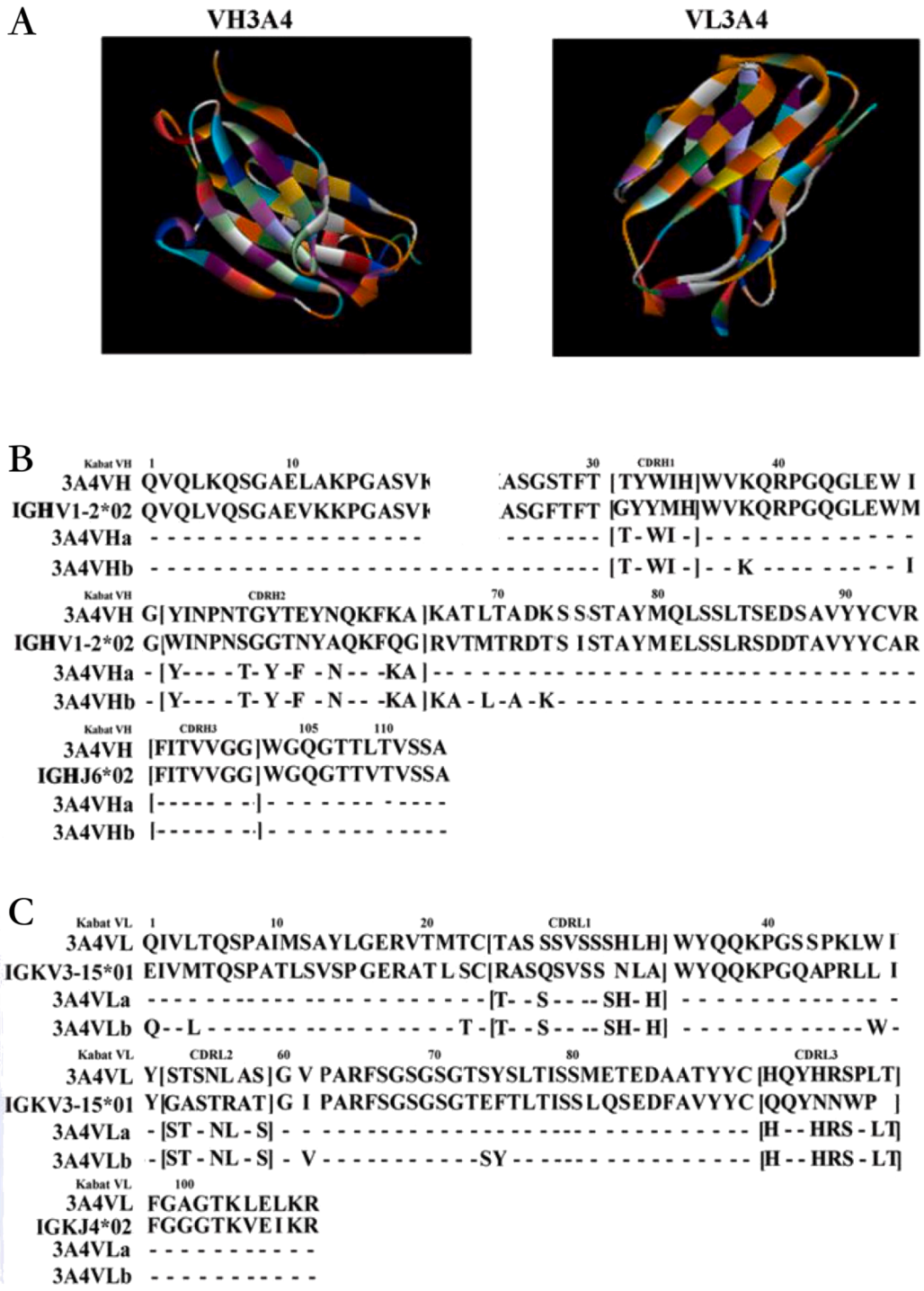

Fig. 1. The 3D modeling and sequence comparison results of the 3A4. (A) The 3D modeling results of the 3A4 heavy and light chain variable regions. Amino acid residues within a 5 Ångström range of the CDR region were identified as key residues using software. (B) Sequence comparison results of the 3A4 heavy chain variable region (3A4VH), human IgG heavy chain variable region (IGHV), and the sequences of key amino acids before (3A4VHa) and after recovery mutation (3A4VHb) in the heavy chain. (C) Sequence comparison results of the 3A4 light chain variable region (3A4VL), human IgG light chain variable region (IGKV), and the sequences of key amino acids before (3A4VLa) and after recovery mutation (3A4VLb) in the light chain.

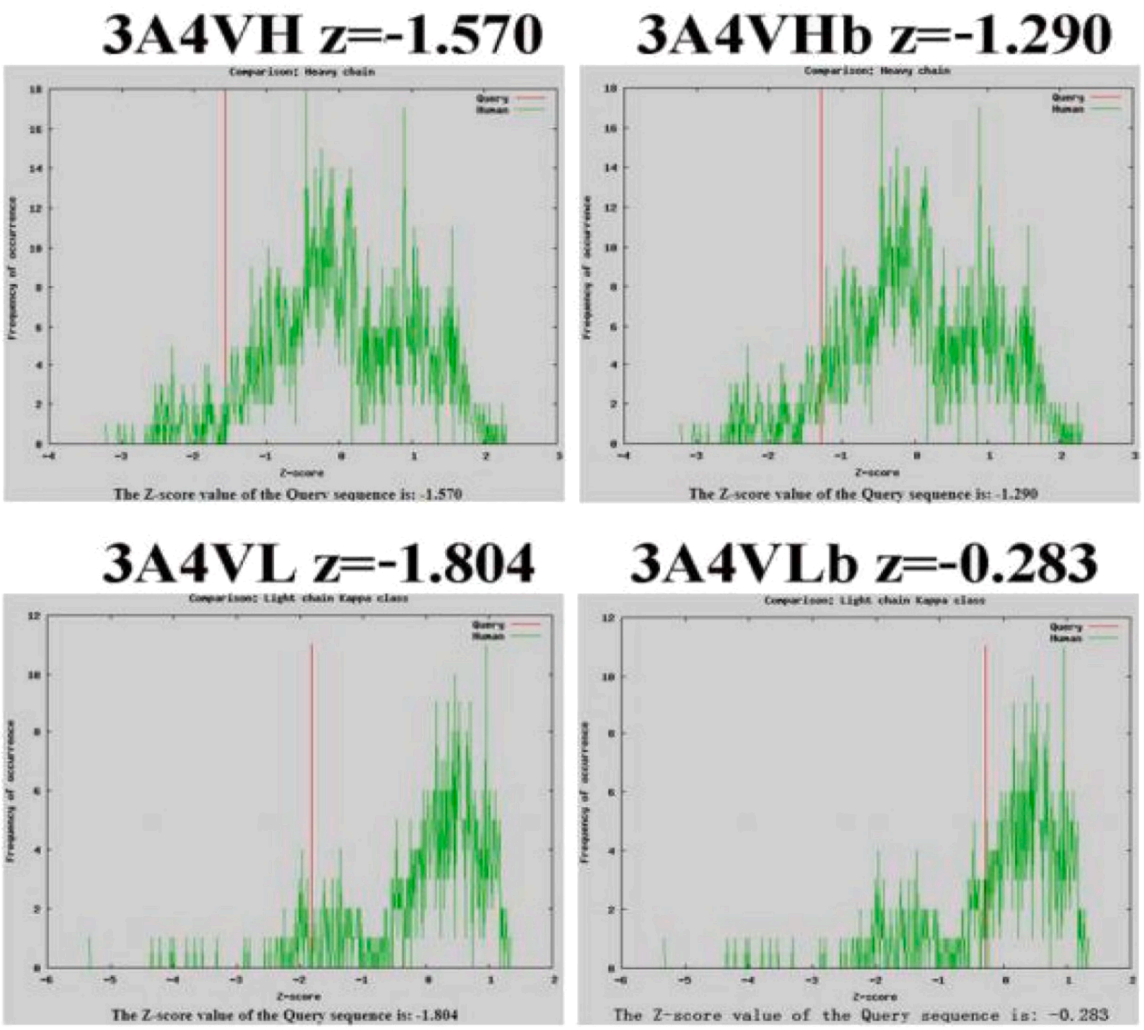

Fig. 2. The design results of the humanized 3A4 antibody.

Expression and purification of the humanized antibody Hu3A4

The expression of Hu3A4 in CHO cells was detected by immunofluorescence microscopy. GAH-k-PE was used to detect the expression of κ light chains in CHO/Hu3A4 cells, and GAH-Fc-FITC was used to detect the expression of the Fc segment in CHO/Hu3A4 cells, with untransfected CHO cells serving as a negative control (blank CHO). Under fluorescence microscopy, red and green fluorescences can be observed in the cytoplasm of CHO/Hu3A4 cells. Merging the images results in a picture with yellow fluorescence, indicating that CHO/Hu3A4 has successfully expressed the recombinant protein. In the CHO control group, no fluorescence was observed (Fig. 3A).

The limited dilution method was employed to subclone the transfected CHO/Hu3A4 cells, resulting in 11 monoclonal cell lines. After expansion, 200 μl of the cell culture supernatant was used for flow cytometry analysis. It was observed that cell lines 3 and 4 exhibited strong expression, with similar percentages of positive cells at 98.08 % and 98.89 %, respectively. However, cell line 3 had a higher median fluorescence intensity of 34.03, compared to 22.43 for cell line 4 (Fig. 3B). Therefore, cell line 3 was selected for further expansion and subsequent functional studies. Purified antibodies were subjected to SDS-PAGE and Western Blot analysis (Fig. 3C), revealing a single band of approximately 160 kDa under non-reducing conditions (without DTT) in lanes 2 and 4, consistent with the theoretical size of Hu3A4.

The binding affinity of Hu3A4

The titration results showed (Fig 4A): With the increase of Hu3A4 antibody concentrations, the positive rate of binding to the antigen gradually reached saturation. A concentration of 0.5 μg Hu3A4 reacting with 1×10^6 KG1a cells achieved a positive cell rate of over 96 %; whereas, to reach a saturated binding rate, approximately 1.0 μg of scFv3A4b-Fc antibody was required.

The competitive binding experiment of Hu3A4 showed (Fig 4B): When the amount of antigen was fixed, with the increase of the amount of Hu3A4, the binding of 3A4 to the antigen gradually decreased. Hu3A4 concentrations of 0.0125 μg, 0.125 μg, 0.25 μg, 0.5 μg, 1.25 μg, 2.5 μg, 5 μg led to a decrease in 3A4 antibody-antigen binding by 0 %, 4.0 %, 7.63 %, 12.16 %, 25.07 %, 32.29 %, 52.45 %, respectively. The regression curve is plotted as the following equation $y = -1.3696x^2 + 16.699x + 2.5791$ (where x is the antibody amount and y is the inhibition rate of antibody-antigen binding, $R^2 = 0.9818$). According to the equation, when the antibody-antigen binding decreases by 50 %, the amount of Hu3A4 is calculated to be 4.502 μg. Based on the amino acid sequence of the Hu3A4 antibody, its protein molecular weight is calculated to be approximately 151kDa, and the amount of 4.502 μg of protein corresponds to approximately 2.683×10^{-11}M. The relative affinity constant is the reciprocal of the molarity, i.e., $Ka = 3.7 \times 10^{10}M^{-1}$. In contrast, the regression curve equation for the scFv3A4b-Fc antibody is $y = -0.1896x^2 + 4.9318x + 0.6661$ (where x is the antibody amount and y is the inhibition rate of antibody-antigen binding, $R^2 = 0.9954$), with its relative

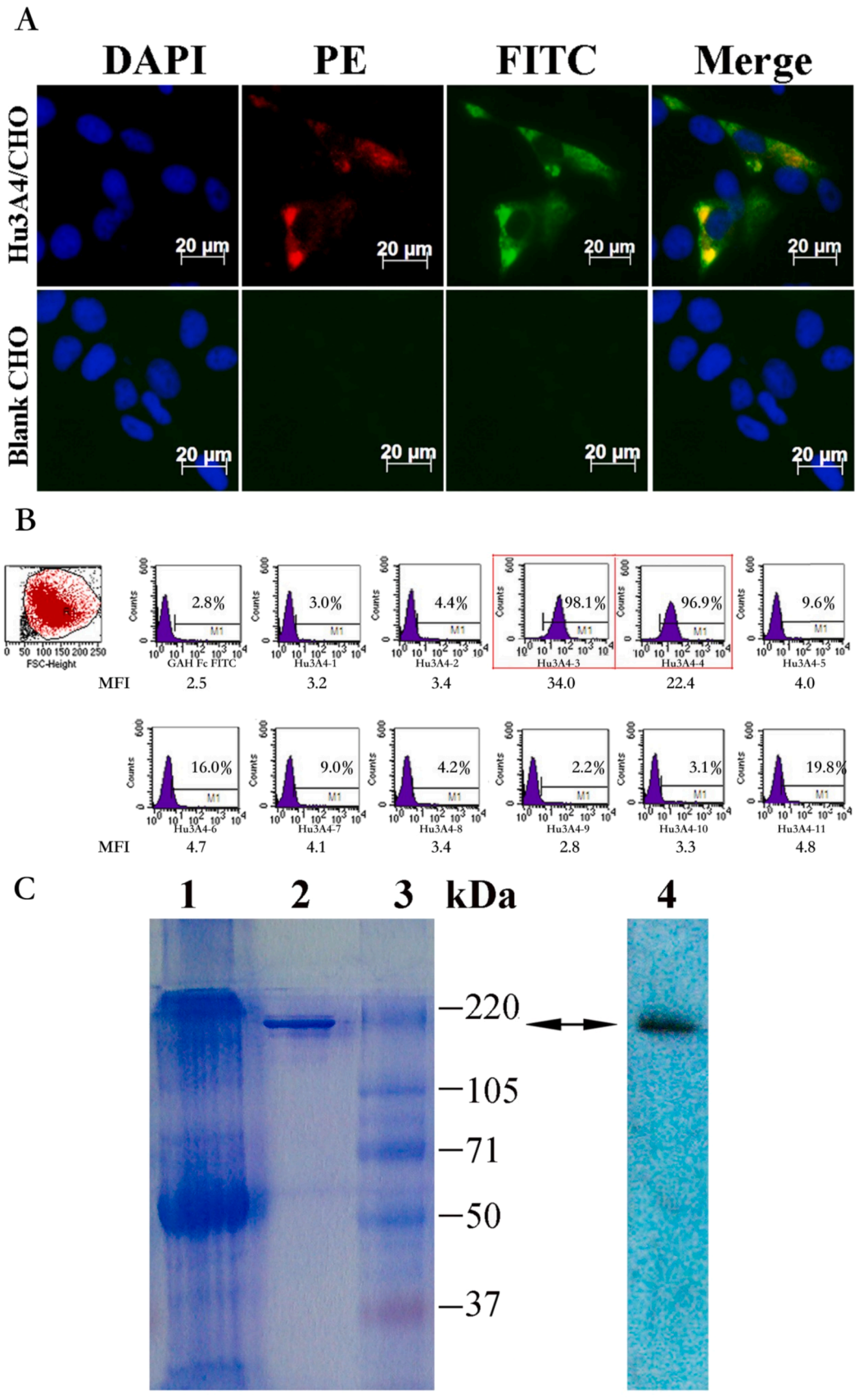

(caption on next page)

Fig. 3. Identification of Hu3A4. (A) Immunofluorescence identification of recombinant protein expression in CHO/Hu3A4 cells. DAPI: labels the cell nucleus; PE: labels the human κ chain; FITC: labels the human Fc fragment; Merge: composite image. Under fluorescence microscopy, red and green fluorescence can be observed in the cytoplasm of CHO/Hu3A4 cells. Merging the images results in a picture with yellow fluorescence, indicating that CHO/Hu3A4 has successfully expressed the recombinant protein. In the control CHO group, no fluorescence was observed. (B) Flow cytometric screening of Hu3A4 cell line subclones, revealing that the positive rate and MFI of this cell line 3 were the highest. (C) SDS-PAGE and Western Blot analysis of Hu3A4 Antibody. Lane 1: Before purification; Lane 2: After purification; Lane 3: Protein marker; Lane 4: Hu3A4 Western Blot result.

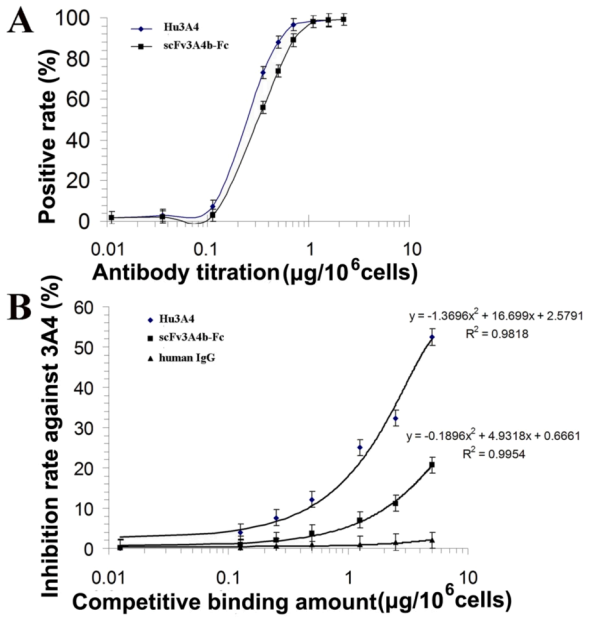

Fig. 4. The binding affinity of Hu3A4. (A) Antibody titration of Hu3A4 and scFv3A4b-Fc. (B) Competitive binding assay results for Hu3A4 and scFv3A4b-Fc.

affinity calculated as Ka=4.7 × 10^9M^{-1}. This indicates that the affinity of Hu3A4 is significantly superior to that of scFv3A4b-Fc.

In vitro antitumor activity of Hu3A4

CDC Effect of Hu3A4 and scFv3A4b-Fc: The CDC impact of Hu3A4 and scFv3A4b-Fc on KG1a cells showed no significant variation across different concentrations. Specifically, at 50 μg/ml, cell lysis rates for Hu3A4 and scFv3A4b-FcHis were 7.46 ± 0.39 and 5.16 ± 0.44, respectively; at 25 μg/ml, 5.63 ± 0.26 vs. 4.16 ± 0.32; and at 10 μg/ml, 4.70 ± 0.21 vs. 3.73 ± 0.38 (all $p > 0.05$) (Fig. 5B). In contrast, using 2E8 as an antibody, about 68 % of target Nalm-6 cells were lysed with only 10 μl of serum complement (Fig. 5A), indicating that the complement system is functional within these experiments while no CDC activity of the antibody was detected.

ADCC Activity of Hu3A4 and scFv3A4b-FcHis Against KG1a Cells: Hu3A4 and scFv3A4b-FcHis effectively induced ADCC-mediated killing of CD45RA positive KG1a cells. Compared to human IgG, Hu3A4 achieved a significant increase in cell lysis at a PBMC:KG1a ratio of 25:1 (41.66 % vs. 4.9 %, $p < 0.05$) and 50:1 (46.8 % vs. 5.1 %, $p < 0.05$). Similarly, scFv3A4b-FcHis showed enhanced lysis rates at the same effector to target ratios, achieving 24.56 % vs. 4.9 % ($p < 0.05$) and 29.5 % vs. 5.1 % ($p < 0.05$), respectively (Fig. 5C). These results confirmed the potent ADCC activities of both antibodies, with efficacy increasing at higher effector to target ratios and Hu3A4 displaying superior ADCC potency compared to scFv3A4b-Fc.

In vivo antitumor activity of Hu3A4

The NOD/SCID xenograft model was employed to evaluate the in vivo anti-tumor efficacy of Hu3A4 over a total observation period of 200

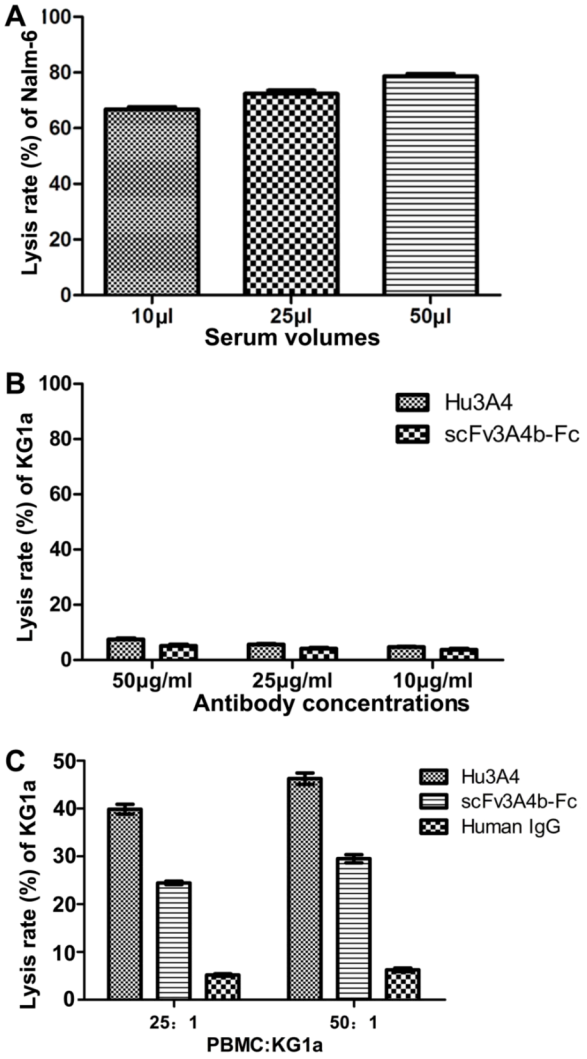

Fig. 5. CDC and ADCC Effects of Hu3A4 and scFv3A4b-Fc. (A) CDC experimental system identify: Lysis rate of Nalm-6 cells by 25 μg/ml 2E8 antibody with varying serum complement volumes (10 μl, 25 μl, 50 μl); (B) CDC activity determination based on lysis of KG1a cells by different concentrations of Hu3A4 and scFv3A4b-Fc. (C) ADCC effects of Hu3A4 and scFv3A4b-Fc on KG1a cells.

days. We observed that mice in the control group survived the entire duration of the study, showcasing a stark contrast to the model group of NOD/SCID mice, all of which died by day 136. In the group treated with Hu3A4, a single mouse passed away on day 161, yet the other four continued to thrive, marking a significant enhancement in survival compared to the model group ($p < 0.05$). The scFv3A4b-Fc treatment group experienced deaths on days 143, 155, 165, 174, and 190, demonstrating each as a notable extension in lifespan against the model group ($p < 0.05$). Importantly, the comparison between the Hu3A4 and scFv3A4b-Fc treatments indicated a significant discrepancy ($p < 0.05$), underscoring the greater therapeutic effect of Hu3A4 in vivo (Fig. 6).

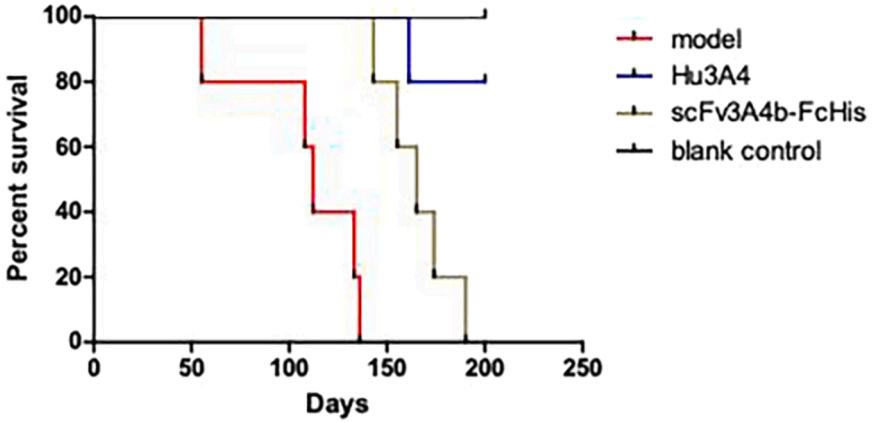

Fig. 6. Survival curves of mice treated with Hu3A4 and scFv3A4b-FcHis.

Discussion

In this study, we have engineered and characterized a humanized full IgG antibody, Hu3A4, manifesting enhanced affinity and superior ADCC capabilities when juxtaposed with the scFv-Fc antibody configuration. Single-chain variable fragment (scFv) antibodies, typically around 25kDa, boast robust tissue penetration yet are hindered by brief systemic half-lives and rapid clearance [21]. Their inability to effectively engage the ADCC and CDC pathways stems from the absence of constant regions. The scFv-Fc constructs with a molecular weight of approximately 105kDa address these limitations by integrating the high affinity and specificity of scFvs with an Fc domain, thereby enabling both ADCC and CDC functions. Both scFv and scFv-Fc antibodies, are noted for their ease of expression and purification, making them valuable approaches across imaging diagnosis [22,23], antiviral [24,25] and antitumor therapies [26–29].

Despite some reports suggesting comparable antigen-binding affinities between scFv-Fc antibodies and their full IgG counterparts, it is widely recognized that scFv-Fc constructs exhibit the reduced affinity. This observation is exemplified by studies, such as those conducted by West et al., indicating a markedly diminished neutralizing efficacy against HIV-1 by scFv-Fc antibodies, likely attributable to their inferior binding affinity towards the HIV antigen [30]. Furthermore, the linker peptide within scFv configurations may introduce new antigenic determinants, with its length critically impacting the overall affinity of scFv-Fc antibodies. In clinical settings, the meticulous design of the linker peptide length is imperative to mitigate immunogenicity while preserving binding affinity [31].

To circumvent the constraints associated with scFv-Fc antibodies, the present study has developed the full IgG antibody Hu3A4. Echoing the observations of West and colleagues, Hu3A4 showcased a notably higher affinity compared to its scFv3A4b-Fc equivalent. This enhanced affinity is likely due to the suboptimal length and structure of the linker peptide in scFv3A4b and the more physiologically relevant configuration of Hu3A4, facilitating the formation of antigen-antibody complexes in a more energetically favorable state. Consequently, this structural optimization has led to a significant elevation in affinity, underscoring the therapeutic potential of full IgG formulations in advancing antibody-based interventions.

CDC and ADCC constitute pivotal immune mechanisms through which antibodies specifically target and eliminate cells [32–34]. CDC activation occurs upon antibody binding to its corresponding antigen on the cell membrane, initiating the classical complement pathway and culminating in the formation of a membrane attack complex that lyses the target cell. ADCC is mediated by effector cells such as natural killer (NK) cells, macrophages, and neutrophils, which identify antibody-coated pathogens or abnormal cells via surface Fc receptors and subsequently neutralize these targets using a variety of mediators, including lysozymes, perforins, tumor necrosis factors, and granzymes [35]. Certain antibodies, like Rituximab—a chimeric anti-CD20 monoclonal antibody marketed as Rituxan—trigger both CDC and ADCC responses by binding to CD20-expressing B lymphocytes in lymphoma patients, leading to tumor cell lysis [36,37]. Conversely, other antibodies, such as trastuzumab (Herceptin) for breast cancer and cetuximab for colon cancer treatment, primarily mediate their therapeutic effects through ADCC [38].

The Hu3A4 antibody developed in this study demonstrated limited CDC activity, likely attributed to the Fc segment's diminished affinity for complement C1q. Studies showed that introducing five point mutations (S267E/H268F/S324T/G236A/I332E) into the Fc region through genetic engineering can enhance its binding capacity to C1q [39]. To improve the CDC activity of Hu3A4, it may be worthwhile to explore the aforementioned approach. In vitro assays revealed that both Hu3A4 and scFvb-Fc antibodies exhibit effective ADCC against target cells, with Hu3A4 displaying notably higher targeted killing capacity, presumably due to its increased affinity for target cells. Further enhancement of Hu3A4′s ADCC function might be achieved through protein engineering (amino acid substitutions S239D/A330L/I332E) or glycoengineering (elimination of core fucose), aiming to augment the Fc segment's affinity for CD16a and thereby bolstering the effector cell-mediated cytotoxicity [40]. Nevertheless, even without modifications to the Fc segment, Hu3A4 and scFv3A4b-Fc antibodies hold potential clinical value, as evidenced by their significant extension of survival in leukemia mouse models.

While full antibodies demonstrate enhanced immunotoxic effects on target cells compared to scFv-Fc constructs, the reduced molecular weight of the latter enables access to antigenic epitopes that are inaccessible to full antibodies, thereby offering a more effective therapeutic strategy for certain intractable and recurrent diseases. Consequently, a balanced exploration of both antibody formats is justified. In another study we published, we described a rapid screening method for humanization, wherein scFv-EGFP fusion proteins facilitate the intuitive and swift identification of single-chain antibodies with antigen-binding activity. This method serves as a foundation for the construction of scFv-Fc and full IgG antibodies, marking a significant stride forward in antibody engineering. In conclusion, this study has successfully developed the fully humanized Hu3A4 antibody, which exhibits considerable ADCC activity and prevents the onset of leukemia in animal models, thus establishing it as a potential candidate for further clinical investigation in the treatment of leukemia.

CRediT authorship contribution statement

Sisi Li: Conceptualization, Formal analysis, Funding acquisition, Writing – original draft, Writing – review & editing. **Zhujun Wang:** Conceptualization, Data curation, Funding acquisition, Methodology.

Xiaoping Guo: Methodology. **Yongmin Tang:** Conceptualization, Supervision, Funding acquisition.

Declaration of competing interest

The authors declare that they have no known competing financial interests or personal relationships that could have appeared to influence the work reported in this paper.

Acknowledgements

This study was supported in part by grants from the National Natural Science Foundation of China (No. 81170502; No. 81300400), and Medical Science and Technology Project of Zhejiang Province (No. 2022KY1051; No. 2013KYA107) and the Scientific Research Foundation of Hangzhou City University (J-202103).

Supplementary materials

Supplementary material associated with this article can be found, in the online version, at doi:10.1016/j.neo.2024.101084.

References

[1] P. Stelmach, A. Trumpp, Leukemic stem cells and therapy resistance in acute myeloid leukemia, Haematologica 108 (2) (2023) 353–366.
[2] K. Mitchell, U. Steidl, Targeting immunophenotypic markers on leukemic stem cells: how lessons from current approaches and advances in the leukemia stem cell (LSC) model can inform better strategies for treating acute myeloid leukemia (AML), Cold Spring Harb. Perspect. Med. 10 (1) (2020).
[3] D. Damiani, M. Tiribelli, Present and future role of immune targets in acute myeloid leukemia, Cancers (Basel) 15 (1) (2022).
[4] T. Manser, et al., The roles of antibody variable region hypermutation and selection in the development of the memory B-cell compartment, Immunol. Rev. 162 (1998) 183–196.
[5] H.R. Hoogenboom, Selecting and screening recombinant antibody libraries, Nat. Biotechnol. 23 (9) (2005) 1105–1116.
[6] H.A. Parray, et al., Hybridoma technology a versatile method for isolation of monoclonal antibodies, its applicability across species, limitations, advancement and future perspectives, Int. Immunopharmacol. 85 (2020) 106639.
[7] M.S. Kinch, Z. Kraft, T. Schwartz, Monoclonal antibodies: Trends in therapeutic success and commercial focus, Drug Discov. Today 28 (1) (2023) 103415.
[8] P. Holzlohner, K. Hanack, Generation of murine monoclonal antibodies by hybridoma technology, J. Vis. Exp. (119) (2017).
[9] L. Mallbris, et al., Molecular insights into fully human and humanized monoclonal antibodies: what are the differences and should dermatologists care? J. Clin. Aesthet Dermatol. 9 (7) (2016) 13–15.
[10] K. Basu, et al., Why recombinant antibodies - benefits and applications, Curr. Opin. Biotechnol. 60 (2019) 153–158.
[11] C.M. Pabon, H.A. Abbas, M. Konopleva, Acute myeloid leukemia: therapeutic targeting of stem cells, Expert Opin. Ther. Targets 26 (6) (2022) 547–556.
[12] B. Kersten, et al., CD45RA, a specific marker for leukaemia stem cell subpopulations in acute myeloid leukaemia, Br. J. Haematol. 173 (2) (2016) 219–235.
[13] R. Joudinaud, T. Boyer, Stem cells in myelodysplastic syndromes and acute myeloid leukemia: first cousins or unrelated entities? Front. Oncol. 11 (2021) 730899.
[14] S. Li, et al., 3A4, a new potential target for B and myeloid lineage leukemias, J. Drug Target 19 (9) (2011) 797–804.
[15] S. Li, et al., Construction, expression, and characterization of a novel human-mouse chimeric antibody, Hm3A4: a potential therapeutic agent for B and myeloid lineage leukemias, DNA Cell Biol. 37 (9) (2018) 778–785.
[16] S. Li, et al., Potent anti-tumor activity of CD45RA-targeting Hm3A4-Ranpirnase against myeloid lineage leukemias, Bioengineered 13 (4) (2022) 8631–8642.
[17] J.H. Kim, H.J. Hong, Humanization by CDR grafting and specificity-determining residue grafting, Methods Mol. Biol. 907 (2012) 237–245.
[18] J. Foote, G. Winter, Antibody framework residues affecting the conformation of the hypervariable loops, J. Mol. Biol. 224 (2) (1992) 487–499.
[19] K.R. Abhinandan, A.C. Martin, Analyzing the "degree of humanness" of antibody sequences, J. Mol. Biol. 369 (3) (2007) 852–862.
[20] J. Yang, C. Rader, Cloning, expression, and purification of monoclonal antibodies in scFv-Fc format, Methods Mol. Biol. 901 (2012) 209–232.
[21] P. Munoz-Lopez, et al., Single-chain fragment variable: recent progress in cancer diagnosis and therapy, Cancers (Basel) 14 (17) (2022).
[22] A. Banisadr, et al., Production of a germline-humanized cetuximab scFv and evaluation of its activity in recognizing EGFR- overexpressing cancer cells, Hum. Vaccin. Immunother. 14 (4) (2018) 856–863.
[23] H.Y. Kim, et al., Development of a SARS-CoV-2-specific biosensor for antigen detection using scFv-Fc fusion proteins, Biosens. Bioelectron. 175 (2021) 112868.
[24] R.T. van Dorsten, et al., Single-chain variable fragments of broadly neutralizing antibodies prevent HIV cell-cell transmission, J. Virol. 96 (4) (2022) e0193421.
[25] A. Sokolowska-Wedzina, et al., High-affinity internalizing human scFv-Fc antibody for targeting FGFR1-overexpressing lung cancer, Mol. Cancer Res. 15 (8) (2017) 1040–1050.
[26] A. Borek, et al., Generation of high-affinity, internalizing anti-FGFR2 single-chain variable antibody fragment fused with Fc for targeting gastrointestinal cancers, PLoS One 13 (2) (2018) e0192194.
[27] M. Sioud, et al., Development of a new high-affinity human antibody with antitumor activity against solid and blood malignancies, FASEB J. 32 (9) (2018) 5063–5077.
[28] C.C. Huang, et al., RGD4C peptide mediates anti-p21Ras scFv entry into tumor cells and produces an inhibitory effect on the human colon cancer cell line SW480, BMC Cancer 21 (1) (2021) 321.
[29] A.P. West Jr., et al., Single-chain Fv-based anti-HIV proteins: potential and limitations, J. Virol. 86 (1) (2012) 195–202.
[30] M. Arslan, et al., Effect of non-repetitive linker on in vitro and in vivo properties of an anti-VEGF scFv, Sci. Rep. 12 (1) (2022) 5449.
[31] P. Shrestha, et al., Daratumumab induces cell-mediated cytotoxicity of primary effusion lymphoma and is active against refractory disease, Oncoimmunology 12 (1) (2023) 2163784.
[32] H.J. van der Horst, et al., Fc-engineered antibodies with enhanced Fc-effector function for the treatment of B-cell malignancies, Cancers (Basel) 12 (10) (2020).
[33] A. Natsume, R. Niwa, M. Satoh, Improving effector functions of antibodies for cancer treatment: enhancing ADCC and CDC, Drug Des. Devel. Ther., 3 (2009) 7–16.
[34] P. Desroys du Roure, et al., A novel Fc-engineered cathepsin D-targeting antibody enhances ADCC, triggers tumor-infiltrating NK cell recruitment, and improves treatment with paclitaxel and enzalutamide in triple-negative breast cancer, J. Immunother. Cancer 12 (1) (2024).
[35] O. Manches, et al., In vitro mechanisms of action of rituximab on primary non-Hodgkin lymphomas, Blood 101 (3) (2003) 949–954.
[36] J. Arora, et al., T cell help in the tumor microenvironment enhances rituximab-mediated NK cell ADCC, Blood (2024).
[37] F. Li, S. Liu, Focusing on NK cells and ADCC: A promising immunotherapy approach in targeted therapy for HER2-positive breast cancer, Front. Immunol. 13 (2022) 1083462.
[38] S. Rosskopf, et al., Enhancing CDC and ADCC of CD19 antibodies by combining Fc protein-engineering with Fc glyco-engineering, Antibodies (Basel) 9 (4) (2020).
[39] R. Repp, et al., Combined Fc-protein- and Fc-glyco-engineering of scFv-Fc fusion proteins synergistically enhances CD16a binding but does not further enhance NK-cell mediated ADCC, J. Immunol. Methods 373 (1-2) (2011) 67–78.
[40] Z. Wang, et al., Successful construction and stable expression of an anti-CD45RA scFv-EGFP fusion protein in Chinese hamster ovary cells, Protein Expr. Purif. 94 (2014) 1–6.